

# Tribological behavior of SiC coating on C/C composites against SiC and WC under unlubricated sliding

Chen Zishan, Li Hejun\*, Fu Qiangang, Chu Yanhui, Wang Shaolong, He Zibo

*State Key Laboratory of Solidification Processing, Carbon/Carbon Composites Research Center, Northwestern Polytechnical University, Xi'an 710072, China*

Received 24 July 2012; accepted 9 August 2012

Available online 18 August 2012

## Abstract

In this work, SiC coatings were prepared by chemical vapor deposition on carbon/carbon (C/C) composites. The microstructure and mechanical characteristics of the as-prepared SiC coatings were investigated by scanning electron microscopy, X-ray diffraction and nano-indentation. The tribological behavior of SiC coating was evaluated by a tribometer with a ball-on-disk configuration, applying SiC and WC balls as counterparts with normal contact loads of 2 N, 10 N and 20 N under unlubricated condition. The results of tribological tests show that the friction coefficient of the SiC coating against the SiC ball (SiC/SiC coupling) is lower than that of the SiC coating against the WC ball (SiC/WC coupling) at all tested loads, and the wear volume of SiC coating for the SiC/SiC coupling is lower than that for the SiC/WC coupling by an order of magnitude. A silica film was formed between the contact surfaces for SiC/SiC coupling at 10 and 20 N, which could act as lubrication layer. However, the dominant wear mechanisms of SiC/WC coupling were a mixture of abrasive and fatigue wear.

© 2012 Elsevier Ltd and Techna Group S.r.l. All rights reserved.

**Keywords:** C. Friction; C. Wear resistance; D. Carbides; CVD coating

## 1. Introduction

Carbon/carbon (C/C) composites exhibit excellent high-temperature mechanical properties, low density, and good processability, which are considered as one of the most promising candidate materials for the thermal structure components in aerospace and astronautics applications [1,2]. However, due to the poor anti-wear properties at high temperature, C/C composites show limited applications on the tribological components for advanced engines, such as, the piston, sealing ring and bearings, which highly demands combined excellent property, for instance, superior high-temperature anti-oxidation, high mechanical strength, good abrasive resistance, and low coefficient of friction [3,4]. Wear and oxidation resistant coating is considered an efficient method to address such problems [5–7], it can not only protect the C/C composite from oxidation effectively [8], but also improve their tribological

properties. Among these coatings, SiC coatings show high thermal conductivity, excellent corrosion resistance, good tribological performance and good chemical compatibility with underlying carbon [9–11]. However, previous studies were mainly focused on high temperature anti-oxidation properties [12,13], but the tribological property is hardly mentioned and understood, which is quite crucial in practical application for tribological components. To address this issue, the tribological behavior of C/C composites with SiC coating was investigated in this work.

To understand the tribological behavior under unlubricated conditions, which is the practical application environment for C/C composites, the friction and wear properties were systematically studied using SiC and WC cemented carbide (6 wt% Co) as mating counterparts, which are commonly used as components for thermal structure assemblies and wear resistant applications [14–16]. Firstly, SiC coating was deposited on the surface of C/C composites by chemical vapor deposition (CVD), and the friction coefficient and wear volume of SiC coating dry sliding against SiC and WC balls were measured,

\*Corresponding author. Tel.: +86 29 88495004; fax: +86 29 88492642.  
E-mail address: [lihejun@nwpu.edu.cn](mailto:lihejun@nwpu.edu.cn) (L. Hejun).

respectively. Moreover, the differences of wear mechanisms between the SiC/SiC coupling and the SiC/WC coupling were also illustrated.

## 2. Experimental procedures

The specimens ( $\varnothing$  36 mm  $\times$  8 mm) used as substrates were cut from bulk two dimensional C/C composites with a density of 1.75 g/cm<sup>3</sup>, and hand-abraded using 400, 800 and 1500 grit SiC abrasive papers in turns, then cleaned by ultrasonic with ethanol and dried at 100 °C for 2 h.

SiC coating was deposited on C/C composites by CVD. The furnace was heated to 1000–1100 °C in a gas flow of H<sub>2</sub> and Ar which is respectively used as carrier gas and diluent gas, then Methyltrichlorosilane (MTS) was brought into the reaction section by H<sub>2</sub> bubbling as source, the pressure of reactor was kept at 0.1 MPa, and the deposition time was 4 h.

Unlubricated ball-on-disk experiments were carried out in a tribometer model HT-1000 manufactured by Lanzhou Institute of Chemical Physical. Commercial SiC balls produced by Shanghai Research Institute of Materials with a diameter of 4.76 mm, surface roughness Ra of 0.05  $\mu$ m and hardness of 2100 HV, were used as mating balls. Commercial WC cemented carbide (6 at% Co) balls with a diameter of 4.76 mm, surface roughness Ra of 0.05  $\mu$ m and hardness of 1500 HV, were used as the other mating balls. The sliding tests were performed using three different normal loads of 2 N, 10 N and 20 N, sliding velocity of 0.1 m/s, a slid distance of 720 m and a wear track diameter of 8 mm. All tests were conducted under dry sliding conditions in air with a relative humidity of 50–60% RH and a room temperature of 20–25 °C. Three tests were carried out for each coupling, and the stationary value of friction coefficient was recorded for each test. Finally, the friction coefficients were given as the mean value of the stationary value for each coupling at different loads.

The specific wear volume for balls and coatings was calculated using the following equations:

$$w_b = \frac{\pi d^4}{64R} \quad (1)$$

$$w_d = 2\pi r A \quad (2)$$

where  $R$  is the ball radius,  $d$  is the diameter of the ball wear scar,  $r$  is the disk wear track radius, and  $A$  is the cross-sectional area of wear track on the coating.  $d$  and  $A$  are measured by laser scanning confocal microscopy (OPTE-LICE-C130).

The morphology of SiC coating and wear tracks were observed and analyzed by a scanning electron microscopy (SEM, VEGA TS5136XM) equipped with energy dispersive spectroscopy (EDS, INCA-300). The crystalline structures of SiC coating was analyzed by X-ray diffraction analyzer (XRD, SHIMADZU LIMITED XRD-7000 s). The hardness and elastic modulus of the SiC coating on

C/C composites were measured by nano-indenter (Agilent Nano-indenter G200), employing a diamond Berkovich indenter. The depth was limited to 1  $\mu$ m, and the drift rate was 0.05 nm/s.

## 3. Results and discussion

### 3.1. Characteristics of SiC coating

XRD pattern of the SiC coating obtained by CVD is shown in Fig. 1. The pattern indicates that the coating consists of a dominating phase of  $\beta$ -SiC and a small fraction of  $\alpha$ -SiC (4H type). The driving force for the formation of  $\alpha$ -SiC is not high enough during nucleation stage because of a relatively lower deposition temperature (1000–1100 °C). Zhou [17] reported that the tribological property of  $\beta$ -SiC is better than that of  $\alpha$ -SiC owing to the cracks are more difficult to propagate in  $\beta$ -SiC, implying that the obtained structure would be more favored for anti-wear properties. Fig. 2 shows surface and cross-section SEM images of the SiC coating. It clearly reveals that the coating is about 50  $\mu$ m in thickness, and no obvious crack can be found on surface and cross-section of the coating. The dense structure is good for the anti-wear property and protection of C/C composites against oxidation and the homogeneous structure guarantees the stable tribological behavior. Fig. 2(c) shows EDS analysis of the SiC coating. It can be seen that the atomic ratio of Si:C is approximately 5:4. The surplus Si atom might exist as free silicon or solid solute in SiC. Moreover, the hardness and elastic modulus of the SiC coating are also important properties for its tribological performance. The nano-indentation experiments were performed on the SiC coating, and the hardness and elastic modulus values were obtained as  $28.5 \pm 2$  GPa and  $392.7 \pm 10$  GPa, respectively.

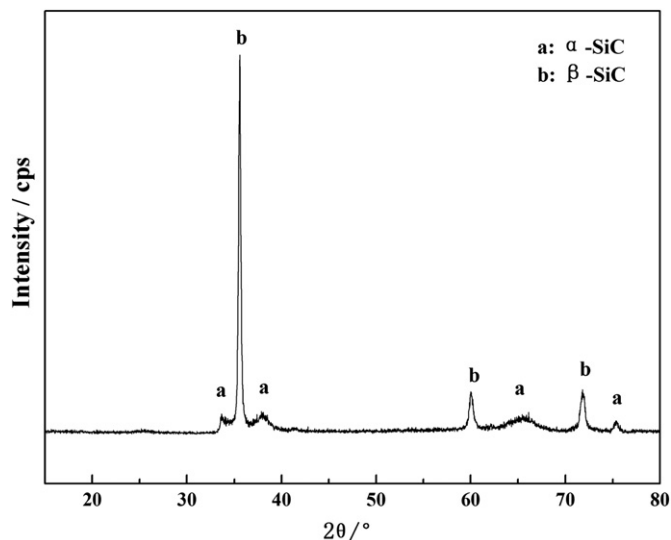


Fig. 1. XRD pattern of the SiC coating obtained by CVD.

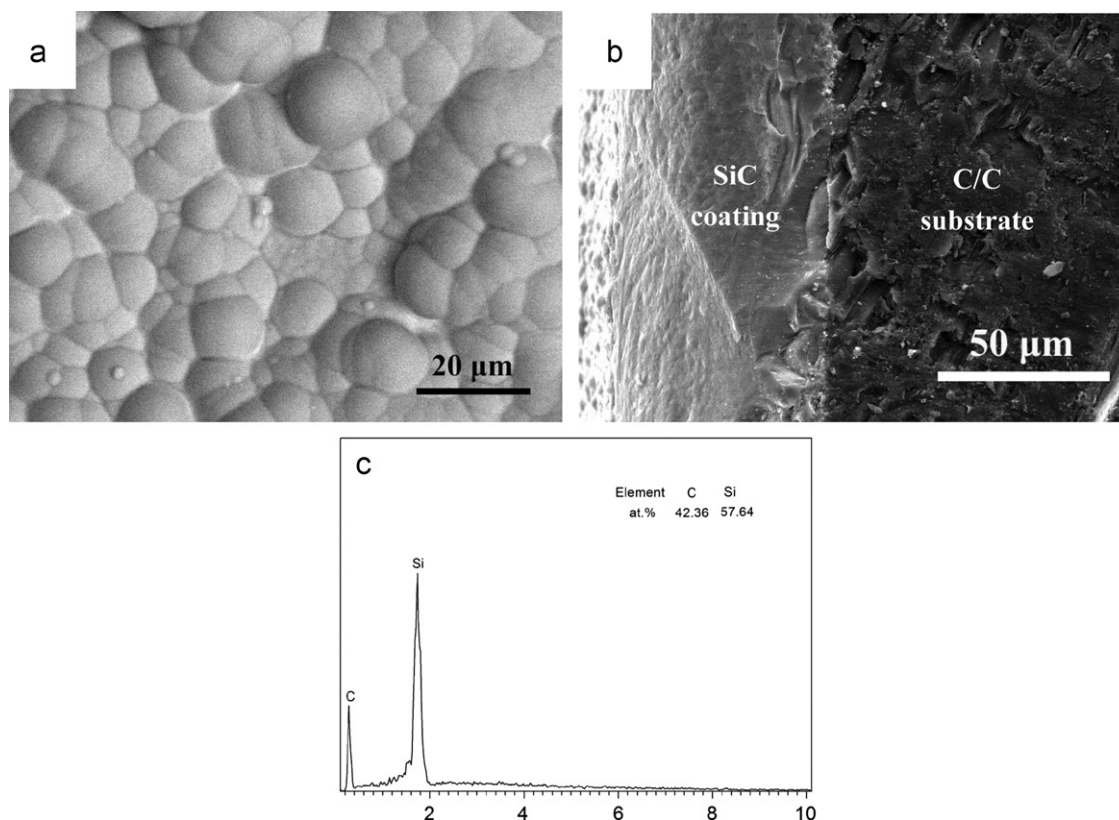


Fig. 2. SEM images and EDS analysis of the SiC coating: (a) surface, (b) cross-section, (c) EDS analysis.

### 3.2. Tribological behavior of SiC coating sliding against SiC balls and WC balls

The friction coefficients of SiC coating sliding against SiC and WC balls under unlubricated condition were evaluated by varying the tested load, as illustrated in Fig. 3. It can be seen that the friction coefficient of the SiC coating against the SiC ball (SiC/SiC coupling) is about 0.40 at 2 N. As the load increases to 10 N, it drops to the lowest value (0.29). However, when the load is 20 N, the friction coefficient of SiC/SiC coupling backs up to about 0.36. As to the SiC coating against the WC ball (SiC/WC coupling), the friction coefficient is 0.45 at 2 N, which is closed to that of SiC/SiC coupling. Whereas, the friction coefficient of SiC/WC coupling increases with increasing the applied load. The friction coefficient is obtained as 0.57 when the load is 10 N, and it is up to 0.68 as the load increases to 20 N. Moreover it is worth noting that the friction coefficient of the SiC/SiC coupling is lower than that of the SiC/WC coupling at all tested loads.

Figs. 4 and 5 show the variation of wear volume of SiC coating and its counterpart for different friction couplings at various tested loads, respectively. For the SiC/SiC coupling, the wear volume of SiC coating (Fig. 4) is  $2.14 \times 10^{-2} \text{ mm}^3$  at 2 N. At 10 N the wear volume of SiC coating is up to  $2.98 \times 10^{-2} \text{ mm}^3$  and then it increases to  $4.96 \times 10^{-2} \text{ mm}^3$  with the load increases to 20 N. For

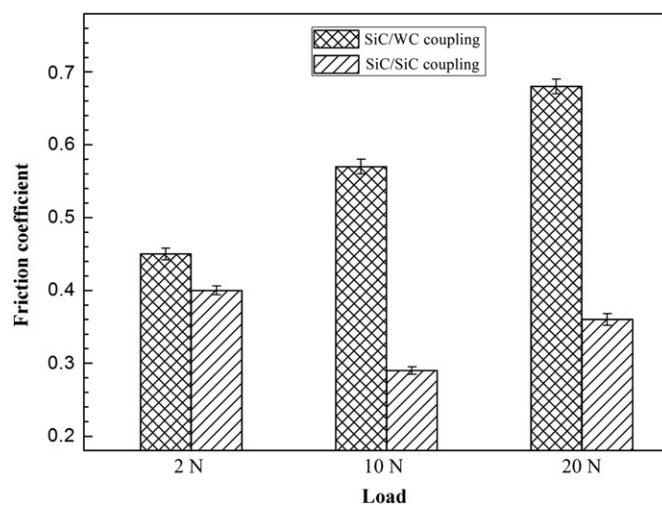


Fig. 3. Friction coefficient of different couplings under tested loads.

the SiC/WC coupling, the wear volume of SiC coating is  $0.11 \text{ mm}^3$  at the load of 2 N and  $0.44 \text{ mm}^3$  at 10 N. As the load increases to 20 N, it rises quickly to  $1.90 \text{ mm}^3$ . It is not surprising that the wear volume of SiC coating increases with the load increases for both tested couplings. However, the wear volume of SiC coating for the SiC/SiC coupling is lower than that of the SiC/WC coupling by an order of magnitude. However, as to the counterparts, the variation of wear volume at various tested loads shows

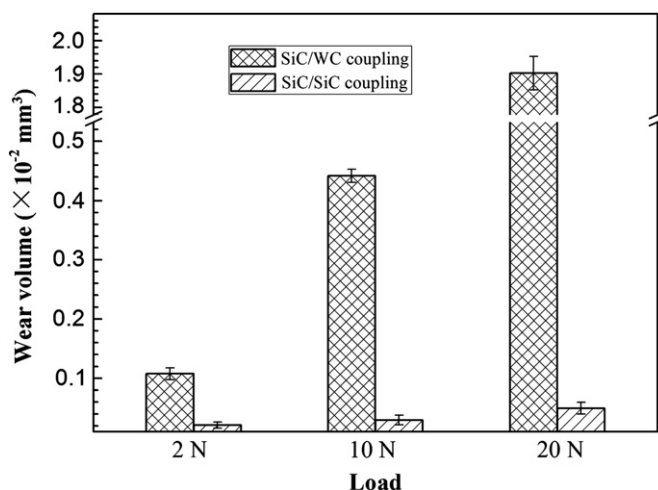


Fig. 4. Wear volume of the SiC coating for different couplings under tested loads.

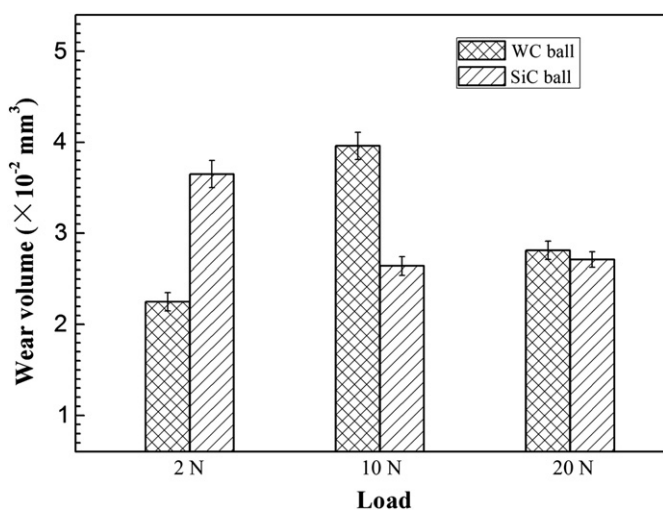


Fig. 5. Wear volume of SiC ball and WC ball under tested loads.

different features. As shown in Fig. 5, the wear volume of SiC ball is  $3.65 \times 10^{-2} \text{ mm}^3$  at 2 N, but decreases slightly to  $2.64 \times 10^{-2} \text{ mm}^3$  at 10 N and rises a little to  $2.71 \times 10^{-2} \text{ mm}^3$  at 20 N. It can be seen that the variation of SiC wear volume with load shows a similar trend as that of friction coefficient of SiC/SiC coupling. For the WC ball, the wear volume is  $2.25 \times 10^{-2} \text{ mm}^3$  at 2 N and  $3.96 \times 10^{-2} \text{ mm}^3$  at 10 N. But it is interesting to note that the wear volume of WC ball declines to  $2.81 \times 10^{-2} \text{ mm}^3$  when the load increases to 20 N.

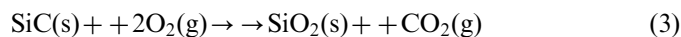
In reviewing aforementioned results, it can be seen that the friction and wear of SiC coating depended largely on the mated materials. The tribological performance of SiC/SiC coupling is more excellent than that of SiC/WC coupling at all tested loads.

### 3.3. Worn surface analysis

SEM images of the worn surface on SiC coating at different tested loads are shown in Figs. 6–10, which will

be beneficial to reveal the wear mechanisms. Fig. 6(a) shows the worn surface on SiC coating for SiC/SiC coupling at 2 N. It can be seen that a wide and shallow wear track generated on the worn surface of SiC coating. A more detailed view of the wear track (in a higher magnification) reveals that the wear track is covered with SiC debris except several unworn regions. It means that the SiC ball counterpart just polished the protruding parts of the SiC coating surface under low-load. Nevertheless, the worn surface of the SiC coating which slides against WC ball at 2 N exhibits a different appearance compared to that of SiC/SiC coupling. As demonstrated in Fig. 6(b), triboislands and flat regions are the main characteristics of the worn surface on the SiC coating for SiC/WC coupling at 2 N. Further observations of the triboislands (the magnification image and EDS analysis) reveal that these triboislands formed from several large debris peeling off the WC ball. As sliding cycle increases, this triboislands would be able to fracture to form second debris which acts as third body accelerating the wear of the coupling. As seen in an amplified image of the flat region which is marked in Fig. 6(b), small grooves can be observed on the worn surface, which should result from the mild abrasive wear caused by WC debris.

Fig. 7 shows the worn surface of SiC coating and its counterpart for the SiC/SiC coupling at 10 N. A thin film can be observed clearly on the worn surface of both the SiC coating and the SiC ball. According to the EDS analysis of these films, an obvious oxygen peak indicates that silica has been generated on worn surface owing to the oxidation of SiC. The oxidation takes place probably by the following reaction:



The reaction is difficult to occur at room temperature, but can be activated owing to the impact of friction [18,19]. According to the previous report [17,20,21], an aggressive loading condition can lead to the elevated temperature generated in the sliding contact surfaces, accelerating the process of oxidation. Therefore, the friction heat promoted oxidation of SiC to form silica. Moreover, the silica film is soft in nature and advantageous for decreasing the friction coefficient [22]. The detailed topographical features of the silica film on the SiC coating are shown in the magnification image in Fig. 7(a). It can be seen that this film covers the worn surface, and the deformation of the film along the sliding direction also can be observed. It reveals that the shear of the film dominated the friction process, which resulted in the decrease of friction coefficient for the SiC/SiC coupling at 10 N.

Fig. 8(a) shows the worn surface of SiC coating sliding against the WC ball at 10 N. It reveals that not only more debris is formed, but also several cracks are emerged on the worn surface. A large crack generated by several small cracks propagation cut across the entire worn surface. The amplified morphology of wear track edge and EDS analysis of this region are also provided in Fig. 8(a), from

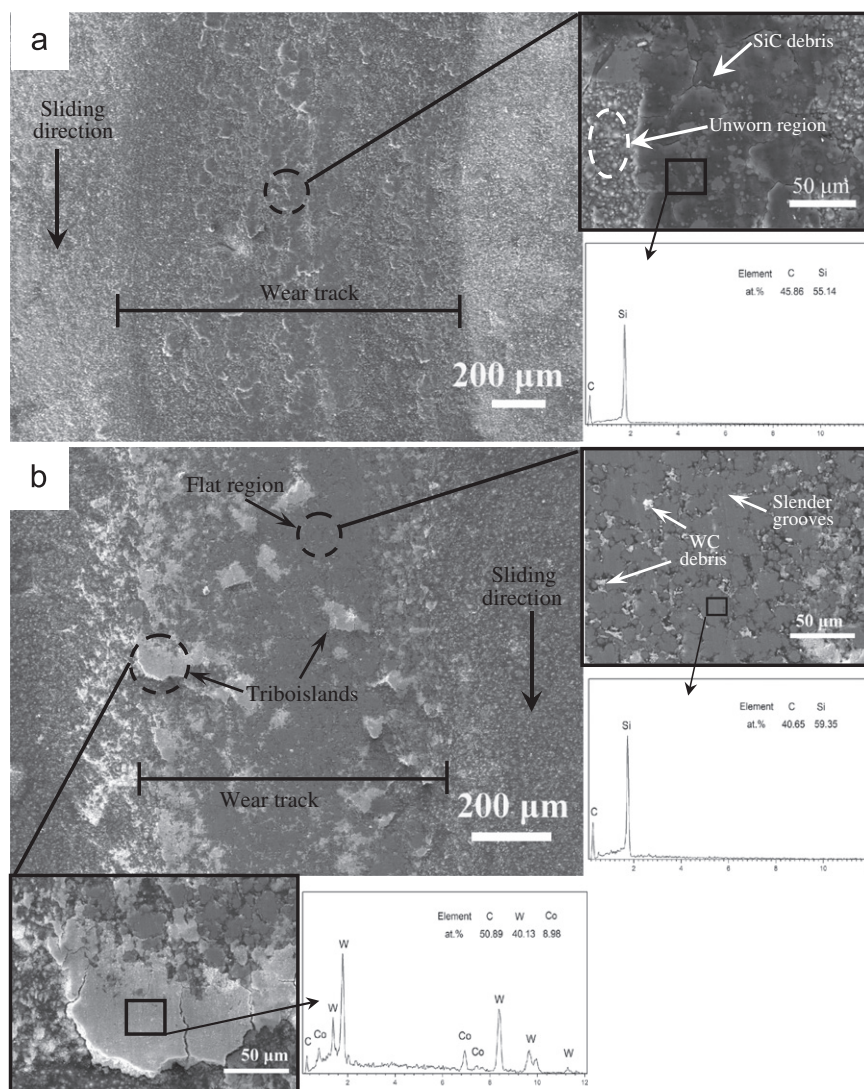


Fig. 6. SEM and EDS analysis of the SiC coating worn surfaces at 2 N: (a) for SiC/SiC coupling, (b) for SiC/WC coupling.

which it can be seen that lots of debris (a few microns in size) congregated around the edge of wear track. This debris is composed of a large number of WC particles and small amounts of oxides according to the EDS analysis. During sliding process, these fine irregular shaped particles can plough the SiC coating just like abrasive grains, causing the presence of grooves on the track, as shown in the magnification image of flat region in Fig. 8(a). Moreover, the analysis of the counterpart can also provide useful insight for the friction process. Fig. 8(b) shows SEM images and EDS analysis of the wear scar on the WC counterpart. It can be seen that the wear scar of the ball is fairly flat except some porous regions. The detailed information of flat and porous regions is shown in magnification images. As seen in the magnification image of the flat region, slender grooves can be observed on the surface. It implied that abrasive wear is one of these wear mechanisms in the friction process. For the porous region, the presence of pores and cracks indicate that grain pullout

and fracture are the main reasons for the wear of porous region. Furthermore, it is worth noting that no oxygen peak was detected on the worn surface of the WC counterpart according to the EDS analysis, which suggested that the oxides in the debris on SiC coating (Fig. 8a) could be silica. Combining with the observations of the SiC coating for SiC/WC coupling at 10 N, a brief description of the friction process is as follows. At the beginning of the test, the generation of debris was closely related to deformation and fracture of asperities on the contact surfaces. Simultaneously, a few of silica was formed on the coating surface owing to the friction heat. Subsequently, more debris is generated as the test went on, and most of this debris is removed to the edge of the wear track. During the removal process, plenty of hard particles (most is WC) resulted in abrasive wear to the worn surfaces and inhibited formation of silica layer. Therefore, abrasive wear is one of the main mechanisms for the SiC/WC coupling at 10 N. It is no wonder that the friction

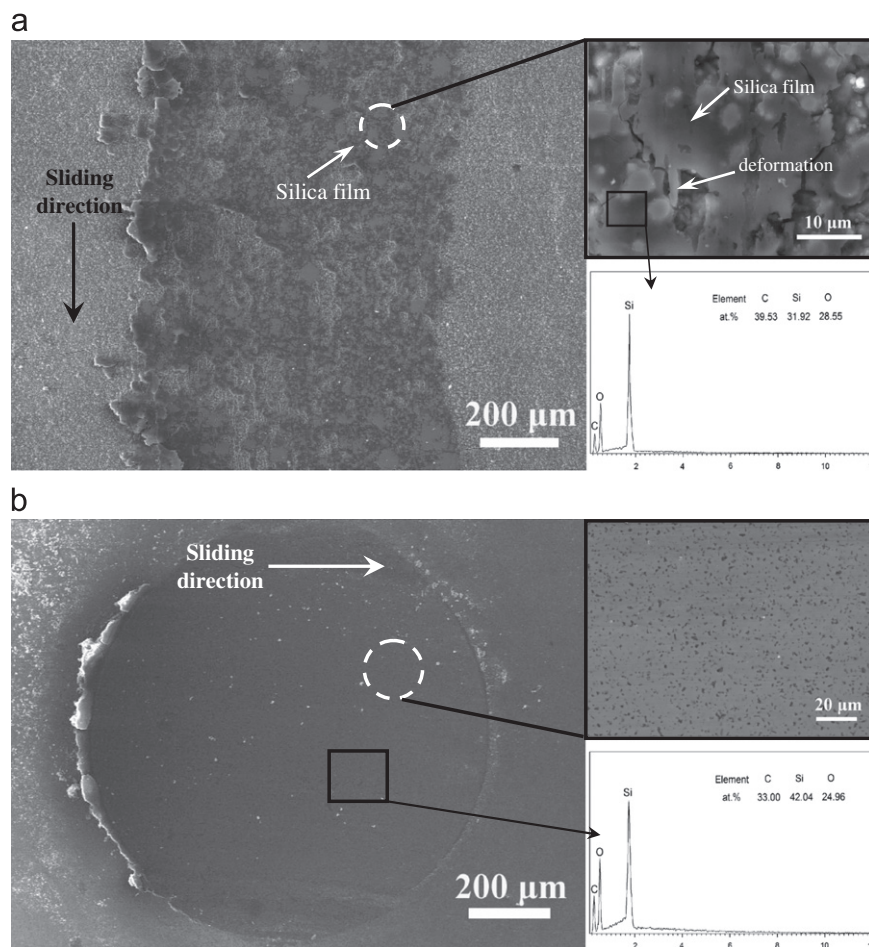


Fig. 7. SEM and EDS analysis of worn surfaces on the SiC/SiC coupling at 10 N: (a) the SiC coating, (b) the SiC ball counterpart.

coefficient of SiC/WC coupling increased from 0.45 to 0.58 with increasing load from 2 N to 10 N. The increase of friction coefficient leads to increase of the tribological stress, and once the stress reaches a critical point, various kinds of cracks can be initiated on the contact surface. In this case, the fatigue wear would dominate the friction process, and different types of cracks can intersect with each other, around the grain boundaries, and across the surface [23]. A further increase of stress will result in fragmentation of the contact surface and more severe wear.

When the load increased to 20 N, for the SiC/SiC coupling, the silica film formed on the coating track is not continuous any more, as shown in Fig. 9(a). It seems that the pressure loaded on the disk exceeds the bearing strength of the silica film, which caused fracture of the film. Even in such condition, the wear scar of SiC ball is still featureless (Fig. 9b), and the wear volume of the ball has little change compared with that under the load of 10 N. However, the fracture of the silica films would weaken its lubricating effect, causing slight rise in friction coefficient. While for the SiC/WC coupling, the evident fragmentation and delamination of the SiC coating and the substrate of C/C composites can be observed in Fig. 10(a). It is easy to understand that more aggressive loading condition resulted

in the fragmentation and delamination of the SiC coating and the formation of more debris, causing fairly high friction coefficient and wear volume of coating. As shown in Fig. 11, more SiC particles are observed in the debris which is collected from the SiC/WC coupling after the friction test at 20 N. They were generated by the breaking of SiC fragment delaminated from the coating, and the size of SiC particles (about 20 μm in size) is larger than that of the WC particles. On one hand, these large particles made deep grooves (Fig. 10b) on the wear scar of the WC ball by abrasive wear and on the other hand, the wear volume of WC ball for SiC/WC coupling at 20 N has obvious decrease due to the failure of SiC coating counterpart.

#### 4. Conclusions

The SiC coating was deposited on C/C composites by CVD, and the tribological behavior of SiC coating sliding against SiC and WC cemented carbide (6 wt% Co) were investigated using a ball-on-disk configuration at room temperature. The results obtained shows that the friction coefficient of the SiC/SiC coupling was lower than that of the SiC/WC coupling at all the test loads, and the wear volume of SiC coating for SiC/SiC coupling was lower than that for SiC/WC coupling by an order of magnitude.

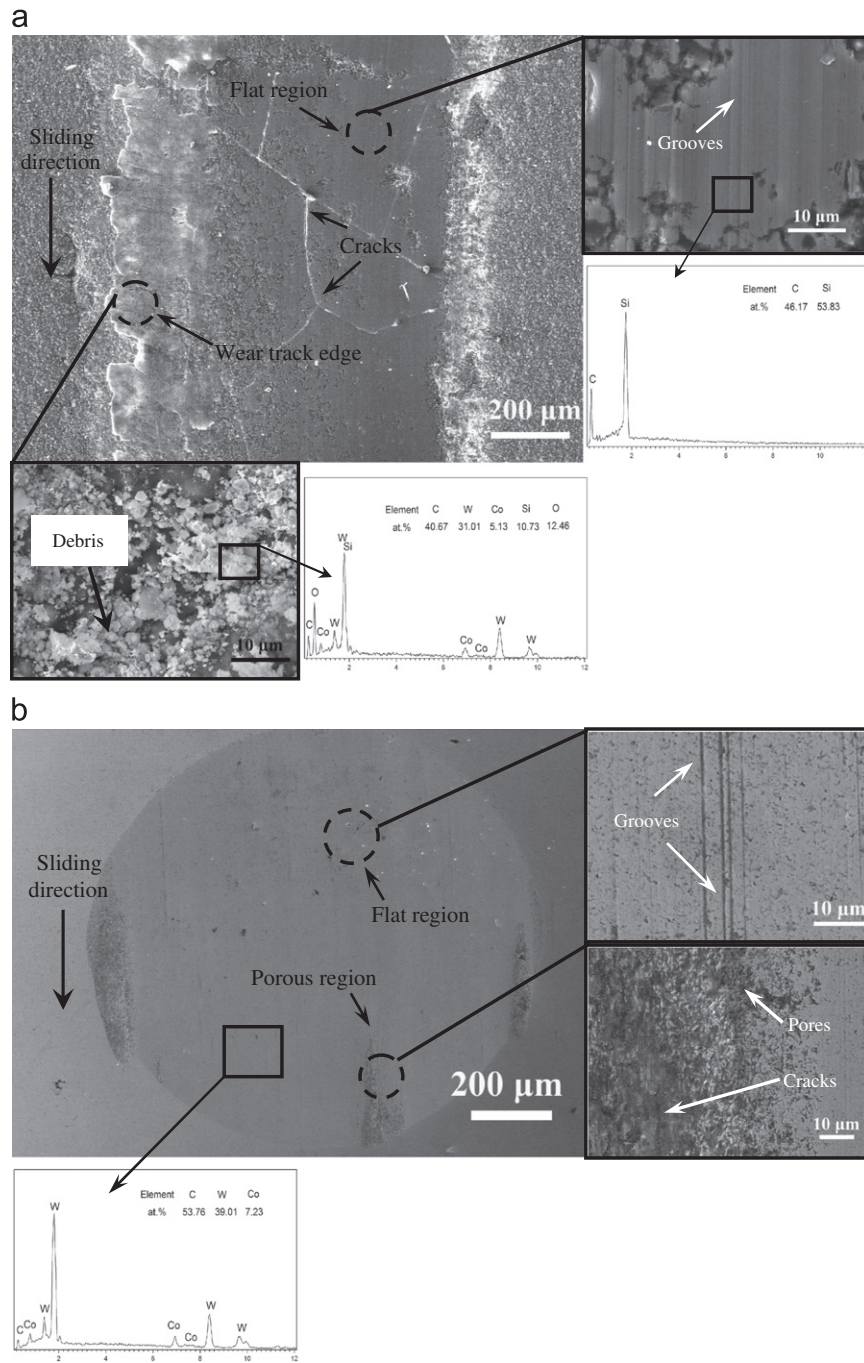


Fig. 8. SEM and EDS analysis of worn surfaces on the SiC/WC coupling at 10 N: (a) the SiC coating, (b) the WC ball counterpart.

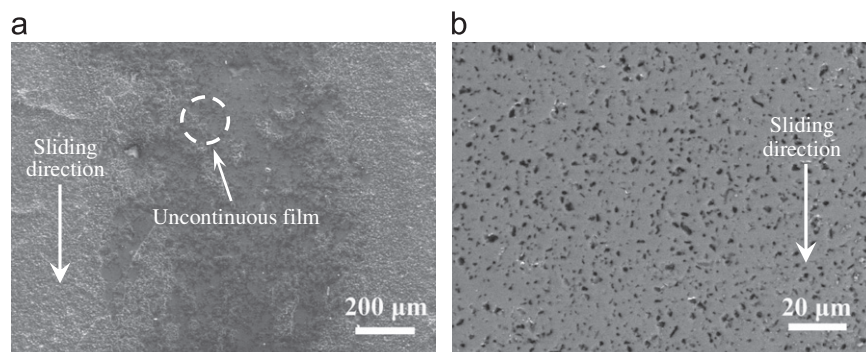


Fig. 9. SEM images of worn surfaces on the SiC/SiC coupling at 20 N: (a) the SiC coating, (b) the SiC ball counterpart.

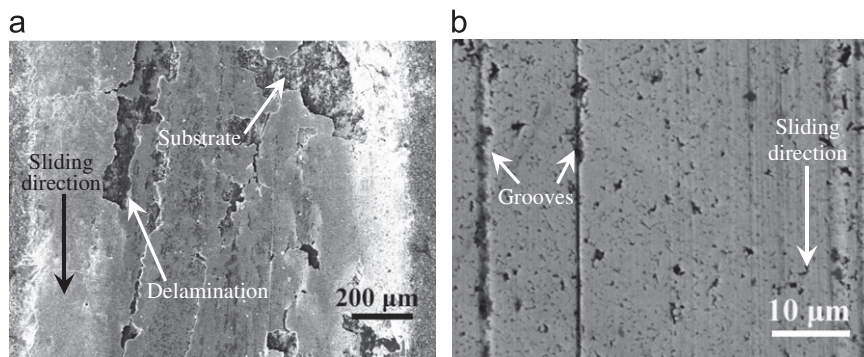


Fig. 10. SEM images of worn surfaces on the SiC/WC coupling at 20 N: (a) the SiC coating, (b) the WC ball counterpart.

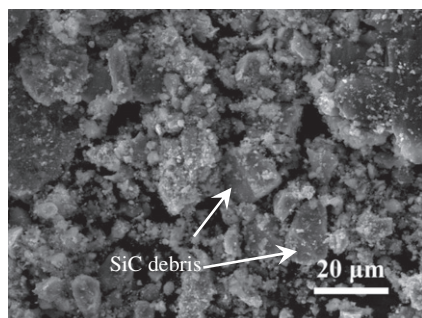


Fig. 11. SEM image of debris for the SiC/WC coupling at 20 N.

For the SiC/SiC coupling, a silica film was formed between the contact surfaces at 10 and 20 N, which is advantageous in the improvement of tribological performance. Nevertheless, the dominant wear mechanisms of SiC/WC coupling were a mixture of abrasive and fatigue wear. The SiC coating was a failure due to the crack propagation and fragmentation while mating with WC ball at 20 N.

## Acknowledgments

This work has been supported by the National Natural Science Foundation of China under Grant nos. 51072166 and 50832004, the Program for New Century Excellent Talents in University, the Research Fund of State Key Laboratory of Solidification Processing (NWPU), China (Grant no. 25-TZ-2009).

## References

- [1] A.V.K. Westwood, B. Rand, S. Lu, Oxidation resistant carbon materials derived from boronated carbon-silicon alloys, *Carbon* 42 (2004) 3071–3080.
- [2] C.A.A. Caio, M. Florian, M.L.A. Graca, J.C. Bressiani, Kinetic study by TGA of the effect of oxidation inhibitors for carbon-carbon composite, *Materials Science & Engineering, A* 358 (2003) 298–303.
- [3] H.J. Li, R.Y. Lou, Z. Yang, The status and future on research and application about carbon/carbon composites in aeronautical area, *Materials Engineering* 8 (1997) 8–10.
- [4] G. Savage, *Carbon/Carbon Composites*, Chapman & Hall, London, 1993.
- [5] F. Smeacetto, M. Ferraris, M. Salvo, S.D. Ellacott, A. Ahmed, R.D. Rawlings, A.R. Boccacini, Protective coating for carbon bonded carbon fibre composites, *Ceramics International* 34 (2008) 1297–1301.
- [6] W. Kowbel, Applications of net-shape molded carbon-carbon composites in IC engines, *Journal of Advanced Materials* 27 (1996) 2–7.
- [7] T. Feng, H.J. Li, Q.G. Fu, Y.L. Zhang, X.H. Shi, Microstructure and anti-oxidation properties of multi-composition ceramic coating for carbon/carbon composites, *Ceramics International* 37 (2011) 79–84.
- [8] C.D. Liu, L.F. Cheng, X.L. Luan, H. Mei, High-temperature fatigue behavior of SiC-coated carbon/carbon composites in oxidizing atmosphere, *Journal of the European Ceramic Society* 29 (2009) 481–487.
- [9] D.A. Rani, Y. Yoshizawa, H. Hyuga, K. Hirao, Y. Yamauchi, Tribological behavior of ceramic materials ( $\text{Si}_3\text{N}_4$ , SiC and  $\text{Al}_2\text{O}_3$ ) in aqueous medium, *Journal of the European Ceramic Society* 24 (2004) 3279–3284.
- [10] Y.L. Zhang, H.J. Li, X.Y. Yao, K.Z. Li, X.F. Qiang, Oxidation protection of C/SiC coated carbon/carbon composites with Si-Mo coating at high temperature, *Corrosion Science* 53 (2011) 2075–2079.
- [11] S.M. Hsu, M. Shen, Wear prediction of ceramics, *Wear* 256 (2004) 867–878.
- [12] B. Wang, K.Z. Li, H.J. Li, Q.G. Fu, SiC coating prepared by a two-step technique of pack cementation and CVD on carbon/carbon composites, *Journal of Inorganic Materials* 22 (2007) 737–741.
- [13] Y.H. Chu, Q.G. Fu, H.J. Li, H. Wu, K.Z. Li, J. Tao, Q. Lei, SiC coating toughened by SiC nanowires to protect C/C composites against oxidation, *Ceramics International* 38 (2012) 189–194.
- [14] V.S.R. Murthy, H. Kobayashi, N. Tamari, S. Tsurekawa, T. Watanabe, K. Kato, Effect of doping elements on the friction and wear properties of SiC in unlubricated sliding condition, *Wear* 257 (2004) 89–96.
- [15] B. Yin, H.D. Zhou, J.M. Chen, X.Q. Zhao, Y.L. An, Comparative study of the friction and wear behavior and wear mechanism of plasma sprayed WC-12%Co coatings matched with ceramic and stainless steel balls under dry sliding condition, *Tribology* 3 (2008) 213–218.
- [16] D.A. Stewart, P.H. Shipway, D.G. Mc Cartney, Microstructural evolution in thermally sprayed WC-Co coatings comparison between nanocomposite and conventional starting powders, *Acta Materialia* 48 (2000) 1593–1604.
- [17] S.Q. Zhou, Research on the Tribological Characteristics of Silocon Carbide and its Composites at High-Temperatures, Doctor Thesis, Hunan University, Changsha, 2006.
- [18] H.N. Xiao, Senda Tetsuya, Plastic deformation and recrystallization of alumina during sliding wear at elevated temperature, *Tribology* 17 (1997) 193–197.

- [19] S.Q. Zhou, H.N. Xiao, Tribo-chemistry and wear map of silicon carbide ceramics, *Journal of the Chinese Ceramic Society* 30 (2002) 641–644.
- [20] F.D. Keith, Wear performance of ceramics in ring/cylinder applications, *Journal of the American Ceramic Society* 72 (1989) 691–695.
- [21] L. Espinosa, V. Bonache, M.D. Salvador, Friction and wear behaviour of WC–Co–Cr<sub>3</sub>C<sub>2</sub>–VC cemented carbides obtained from nanocrystalline mixtures, *Wear* 272 (2011) 62–68.
- [22] Y. Yamamoto, A. Ura, Influence of interposed wear particles on the wear and friction of silicon carbide in different dry atmospheres, *Wear* 154 (1992) 141–150.
- [23] Y.S. Wang, M.H. Stephen, Wear and wear transition mechanisms of ceramics, *Wear* 195 (1996) 112–122.